Optics Communications 285 (2012) 3592–3596

Contents lists available at SciVerse ScienceDirect

Optics Communications

journal homepage: www.elsevier.com/locate/optcom

Highly-efficient optical power combiners based on evanescently-coupled micro/nano optical fibers

Zehua Hong [a], Xinwan Li [a,b,*], Linjie Zhou [a], Weiwen Zou [a], Xiaomeng Sun [a], Shuguang Li [a], Jianguo Shen [a], Haimei Luo [a], Jianping Chen [a]

[a] State Key Laboratory of Advanced Optical Communication Systems and Networks, Department of Electronic Engineering, Shanghai Jiao Tong University, Shanghai 200240, PR China
[b] School of Physics and Electrical Information Science, Ningxia University, Ningxia 750021, PR China

ARTICLE INFO

Article history:
Received 26 February 2012
Received in revised form
17 April 2012
Accepted 17 April 2012
Available online 10 May 2012

Keywords:
Fiber optics components
Micro-optical devices
Microstructure fabrication

ABSTRACT

Novel highly-efficient power combiners based on evanescently-coupled micro/nano optical fibers are proposed and experimentally demonstrated. Experimental results show that the maximum power combing efficiency can be $>90\%$. The combining efficiency is overlap length dependent. As long as the overlap length is long enough ($\sim$7 mm), a stable high combining efficiency can always be achieved. The presented optical power combiners with the advantages of easy fabrication, low-loss, low-cost, and wavelength insensitivity can find potential applications in micro/nano photonic devices, optical communications and optical interconnects.

1. Introduction

In photonics, it is relatively easier to split a light beam into N (N=2, 3, 4, …) beams than to combine multiple beams into a single one. Optical power combination with high coupling efficiency and low cost is a big challenge [1]. So far, there is no simple, low cost, and highly efficient solution to this issue. Moreover, optical power combination is a key technology in many applications from sensing to communications and high power laser fabrication.

Optical power combiners (OPCs) can be used in two broad applications. The first is power scaling of a laser system, that is, a number of lower power beams are combined into a single beam to achieve high output power, which is the high-power level application. Many techniques, both coherent and incoherent, have been reported in power scaling [2–5]. For coherent combination, the phases or/and polarizations of individual beams are controlled, which enables the constructive interference in the combined beams [2,3,6]. Complex structures are usually required for this kind of technologies, which not only increases the cost but also reduces the stability. Incoherent combination, on the other hand, does not require phase or/and polarization control. In Ref. [4], a $(6+1)\times 1$ multimode combiner consisting of six 3 W fiber-coupled pump diodes is employed to provide maximum 18 W pump power. Ref. [5] has demonstrated an all-fiber 7×1 power combiner which couples the output from 7 single-mode fiber lasers into a single multi-mode fiber, and can achieve high combining efficiency of $>95\%$.

Another application is in the low-power level applications. For this type of application, a simple method is to reverse the input and output ports of a splitter to serve as a combiner, as demonstrated in [7]. In their work, a 4×1 multi-mode interferometer (MMI) is used as a power combiner in the hybrid WDM fiber-to-the-x (FTTx, where x indicates home, curb, cabinet, building, etc.). Such kind of power combiners are relatively simple and low-cost, and various structures are employed to construct the OPCs, such as MMIs [7], and Y-branches [8]. However, the combining efficiency is low and sophisticated processing is required to manufacture these structures. Moreover, they also suffer from large coupling losses due to their mode field mismatch to single mode fibers (SMFs).

Micro/nano optical fibers (MNOFs) have proved to be an important medium because they exhibit a number of exciting properties such as large evanescent field, and strong confinement [9,10], which provides opportunities for applications including nonlinear optics [11,12] and micro/nano-scale photonic devices [13–18]. In this letter, we demonstrate highly-efficient optical power combiners (OPCs) based on evanescently-coupled MNOFs. The maximum combining efficiency reaches up to $\sim$90% for both incoherent and coherent light inputs. The proposed OPCs, both incoherent and coherent, can find potential applications in

* Corresponding author at: State Key Laboratory of Advanced Optical Communication Systems and Networks, Department of Electronic Engineering, Shanghai Jiao Tong University, Shanghai 200240, PR China.
E-mail address: lixinwan@sjtu.edu.cn (X. Li).

0030-4018/$ - see front matter Crown Copyright © 2012 Published by Elsevier B.V. All rights reserved.
http://dx.doi.org/10.1016/j.optcom.2012.04.024

"low-power level" optical communications [19] and interconnects [8]. Moreover, we believe the results can also provide valuable references for the design of high-power level optical combiners.

2. Fabrication of OPCs

The $N \times 1$ OPCs were fabricated using a hydrogen flame-heating technique [20]. First, SMFs with their coating stripped were twisted to form a bundle. The fiber bundle was then pulled under a hydrogen flame. The tapering of the MNOFs bundle was controlled by carefully moving the flame and the translation stages where the SMF bundle was attached. With the same approach, we also fabricated a single MNOF. Then we cleaved the MNOF bundles and the single MNOF in the middle (near the minimum waist position), and made them attach with each other in air. Consequently, the MNOFs were tightly bound together because of the Van der Waals and electrostatic forces. A self-aligned OPC was thus formed. Fig. 1(a)–(d) shows the scanning electron microscope (SEM) images of the OPC and its zoomed coupling area including the tapered MNOF bundle consisting of 2, 3, and 4 MNOFs, respectively, and the single MNOF. The waist diameters of the tapered MNOF bundles are ~1 μm and the total lengths including two symmetric tapering regions are about 53, 60, and 66 mm, respectively. The waist diameter and total length of the single MNOF are ~1 μm and 46 mm. Fig. 2(a) shows the schematic configuration of the MNOF-based OPC. Multiple beams were launched into the MNOF bundle from the left side and then coupled into the single MNOF in the overlap section. Finally, light was transmitted out from the right side as a single beam.

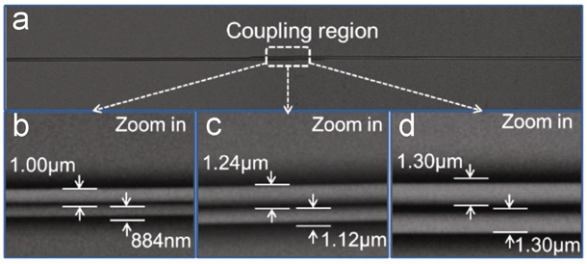

Fig. 1. Scanning electron microscope images of an OPC. (a) Panoramic image of the OPC. (b)–(d) Zoomed-in of the coupling regions in 2×1, 3×1, and 4×1 OPCs. The top waveguides shown in (b)–(d) are the single MNOFs and the bottom waveguides are the MNOF bundles.

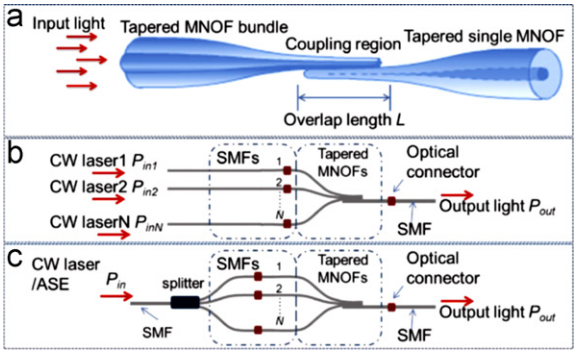

Fig. 2. Schematic diagrams of the OPC and the experimental setup for optical transmission measurement. ASE: amplified spontaneous emission source. (a) Schematic of $N \times 1$ (N=2, 3, 4, …) OPC. The input light can be either incoherent or coherent. (b) and (c) Experimental schemes for incoherent and coherent combination. P_{inN} (N=1, 2, 3, 4, …) is the input power of the Nth beam. Each beam has an equal power level.

3. Experiment and results

Fig. 2(b) shows the experimental setup of the incoherent power combination. Continuous wave (CW) beams from different laser sources with the same wavelength and power level were launched into the input ports of the MNOF-based OPC. It should be noted that all beams are incoherent since they are originated from individual laser sources with relatively random phase variation. Fig. 2(c) shows the schematic illustration of the experimental setup for the coherent power combination. A CW laser source was first divided into N coherent beams by a splitter and then launched into the MNOF-based OPC. It should be noted that phase-locking techniques were not employed in this experiment, and the phase of each beam changed randomly due to the disturbance of external factors. Replacing the CW laser source with an amplified spontaneous emission (ASE) source, the setup shown in Fig. 2(c) can also be used for the incoherent power combining measurement. Here, we define the combining efficiency as $\eta = p_{out}/p_{in}$, where p_{in} and p_{out} are the total input and output optical power respectively. It is noteworthy that the tapered MNOF bundle and single MNOF have a non-negligible insertion loss p_L themselves. In our experiment, the measured insertion losses are ~0.45 dB for the tapered single MNOF and 0.76 dB, 0.93 dB, 1.20 dB for the tapered MNOF bundles consisting of 2, 3, and 4 MNOFs, respectively. In estimating the combining efficiency, the insertion losses of the tapered MNOFs themselves should be taken into account [21]. As a result, the combining efficiency can be rewritten as $\eta = (P'_{out}/P_{in})$, where $P'_{out} = P_{out} + P_L$.

To study the effect of the overlap length on the combining efficiency, we mounted the fiber pigtails of MNOFs of both sides on high precision translation stages. Both MNOFs can be pulled away from each other with an accuracy of 10 μm. Due to the tight binding force between the MNOF bundle and the single MNOF, they do not separate during the pulling process while the overlap length changes.

Fig. 3(a)–(c) shows the measured combining efficiency in incoherent combination as a function of overlap length L at 1550 nm wavelength. The combining efficiency curves are measured using the setup shown in Fig. 2(b). The combining efficiency exhibits a slight oscillation with the overlap length due to the mode beating among MNOF super-modes. When the overlap length is small, the combining efficiency is almost 0. However, when the overlap length increases to several millimeters, the combining efficiency increases very fast and reaches a high value with a weak oscillation. The maximum combining efficiency is ~90% for all OPCs. Fig. 3(a)–(c) also illustrates that, beyond a certain overlap length, almost all the energy from different beams can be transferred from the MNOF bundle to the single MNOF. It implies that, as long as the overlap length is long enough, we can always get a high combining efficiency using our MNOF-based OPC, which can greatly simplify device design and avoid strict alignment.

A broadband light source (e.g. an ASE source) is an ideal incoherent light source. Fig. 3(d)–(f) shows the experimental results in incoherent combination measured by the setup shown in Fig. 2(c) with an ASE source. Similar to the results shown in Fig. 3(a)–(c), the combining efficiency reaches >90% when the overlap length increases to several millimeters. However, the oscillation of the combining efficiency is weaker than that shown in Fig. 3(a)–(c).

In conventional coherent optical combiners, phase-locking is usually used to make the input light beams in-phase to ensure a high combining efficiency. Otherwise, the output optical power will fluctuate with the input phases. Fig. 4(a) shows the output fluctuation in a conventional 2×1 coupler as the coherent OPC without phase-locking. As the phase difference between the two

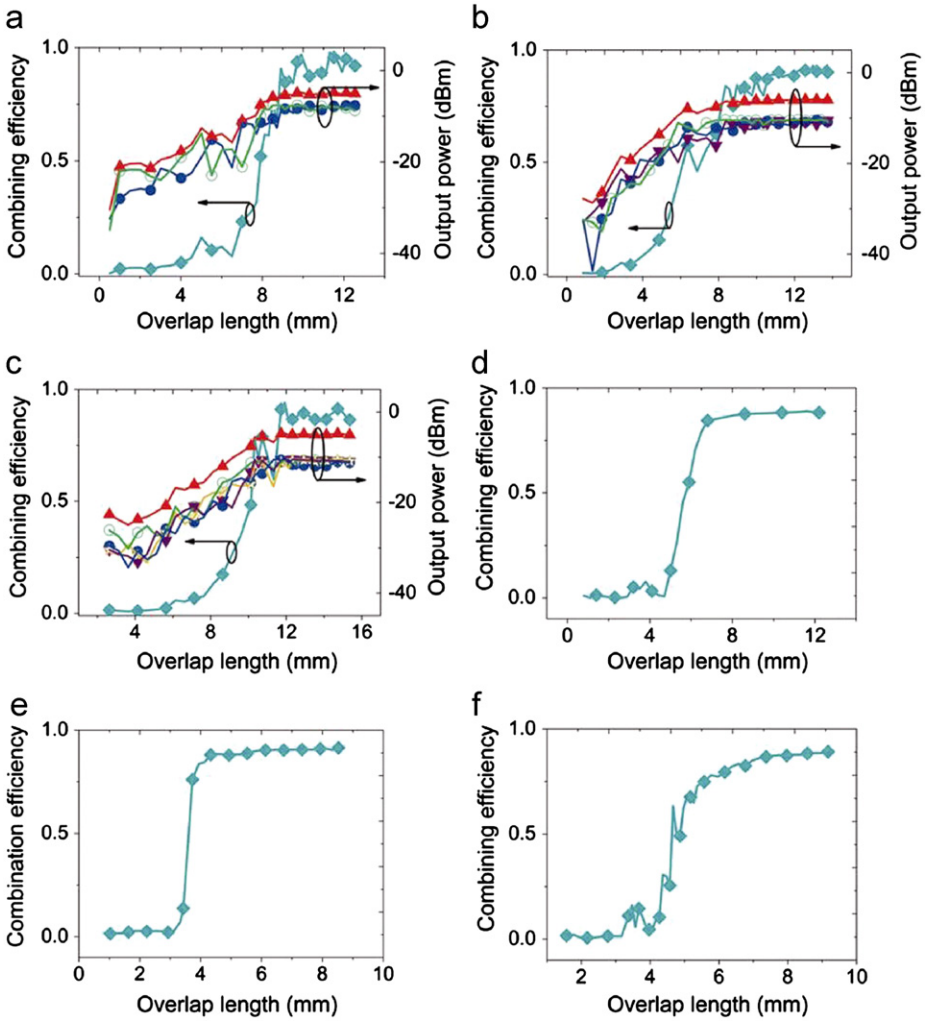

Fig. 3. Measured combining efficiency in incoherent combination as a function of overlap length. (a)–(c) are the combining efficiency curves for 2×1, 3×1, and 4×1 OPCs, respectively, measured by the setup shown in Fig. 2(b). The curves with close diamonds are combining efficiency. Close up-triangles are the output power while all of the lasers are turned on. Other symbols are the output power while only one laser is turned on. (d)–(f) are the combining efficiency curves for 2×1, 3×1, and 4×1 OPCs, respectively, measured by the setup shown in Fig. 2(c) with an ASE source.

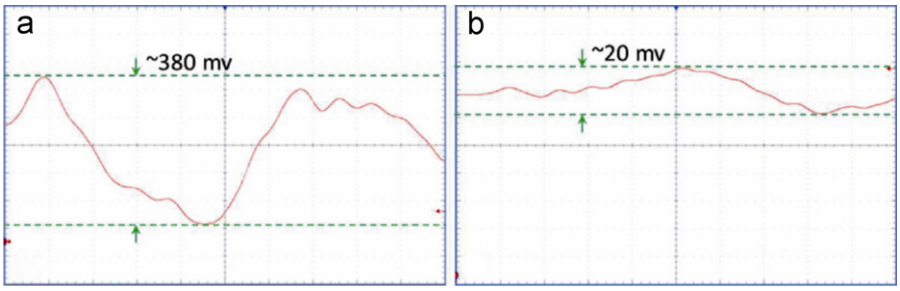

Fig. 4. Time domain waveforms of the output for (a) a conventional 2×1 coupler and (b) a 2×1 OPC proposed in this paper.

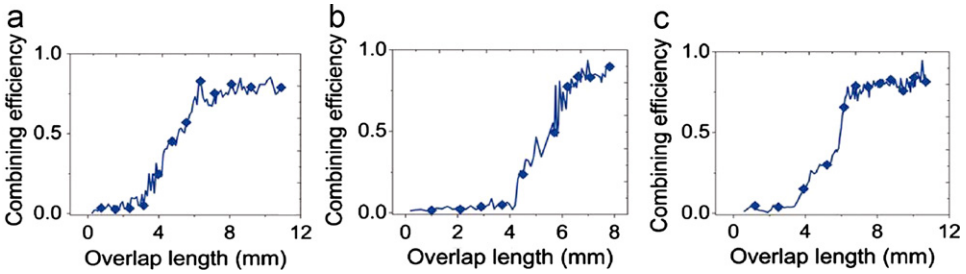

Fig. 5. Measured combining efficiency in coherent combination as a function of overlap length for (a) 2×1, (b) 3×1, and (c) 4×1 OPCs.

arms changes randomly, the output has a large fluctuation of 380 mV [3]. However, the input beam phase variation has much smaller effect on our OPC. As shown in Fig. 4(b), the fluctuation is reduced to 20 mV, more than one order smaller than the previous case. It certifies that coherent optical beams can be combined with a high efficiency even without using any phase-locking technique in our OPC. Fig. 5(a)–(c) shows the measured combining efficiency in coherent combination for $N=2$, 3, and 4, respectively. The combining efficiency changing trend is similar to the incoherent combination case. The maximum combining efficiency is $>85\%$ for the 2×1 OPC, and $>90\%$ for the 3×1 and 4×1 OPCs.

Operation bandwidth is another parameter we should consider in the device design. A broadband light source (Agilent 83438A ERBIUM ASE SOURE) is used to launch light into the 4×1 OPC, and the output spectrum is measured by an optical spectrum analyzer (ANRITSU MS9710B). Fig. 6 shows the normalized output spectrum of the MNOF-based OPC with an overlap length of ~8 mm. we can see the trace shows a slight oscillation with an amplitude of <0.5 dB in the wavelength range of 1510–1590 nm, indicating that the transmission of the OPC is wavelength-insensitive.

4. Discussion

For the coherent combination, in a common sense, the combing efficiency should be low if the phases of all beams entering into the OPC are not matched well [3]. However, our experimental results show that the coupling efficiency of the proposed structure remains high even if the phases of all beams are random. This is because the input MNOFs in the OPC are slightly different in their cross-sectional dimensions, which imposes a different propagation constant β for each beam. Coupled-mode theory can be used to explain the experimental results. The coupled equations for the 2×1 coherent OPC can be approximately described as [22]:

$$\frac{d}{dz}\begin{pmatrix}a_1(z)\\a_2(z)\\a_3(z)\end{pmatrix}=j\begin{pmatrix}\beta_1(z) & k_{21}(z) & k_{31}(z)\\k_{12}(z) & \beta_2(z) & k_{32}(z)\\k_{13}(z) & k_{23}(z) & \beta_3(z)\end{pmatrix}\begin{pmatrix}a_1(0)\\a_2(0)\\a_3(0)\end{pmatrix}, \quad (1)$$

where z is the light propagation distance, $a_1(z)$ and $a_2(z)$ are the amplitudes of the input light beams, $a_3(z)$ is the amplitude of the output light beam, and $\beta_1(z)$, $\beta_2(z)$, and $\beta_3(z)$ are the propagation constants of the corresponding MNOFs, respectively. It should be noted that the propagation constants are no longer constant along the propagation direction, and instead they are assumed to change linearly with z with their changing slopes as s_1, s_2, and s_3. $k_{ij}(z)$ (i, $j=1$, 2, 3) is the coupling coefficient between MNOFs. For simplicity, we assume $k_{ij}(z)$ is a constant.

Fig. 7 shows the simulation results at wavelength $\lambda=1550$ nm. $\Delta\varphi$ is the phase difference between the two input light beams. For Fig. 7(a) and (b), we assume the geometric parameters of the two input MNOFs are slight different, then $\beta_1(0)$, $\beta_2(0)$, and $\beta_3(0)$ are set to be 5.43, 5.35, and 4.42 rad/μm, and s_1, s_2, s_3 are set to be $-1.35e-4$, $-1.35e-4$, and $1.3e-4$. It shows the output power remains high while $\Delta\varphi$ varies from 0° to 180°, which is in agreement with the experimental results. In Fig. 7(c), we assume the two input MNOFs have the same geometric parameters, that is $\beta_1(0)=\beta_2(0)$ and $s_1=s_2$. When the two input ports are out of phase ($\Delta\varphi=180^\circ$), there is almost no output light as shown by the dash line. In contrast, when they are in phase ($\Delta\varphi=0^\circ$), almost all the optical energy can be transferred to the output port as illustrated by the solid curve.

As mentioned, the proposed OPCs can find applications in optical communications and interconnects due to their key merits of easy fabrication, high combining efficiency, wavelength-insensitivity, and low cost. In the application of high power fiber lasers, the power level is very high, which may damage the proposed device. However, we believe the results can provide valuable references for power combiner design in high power fiber lasers.

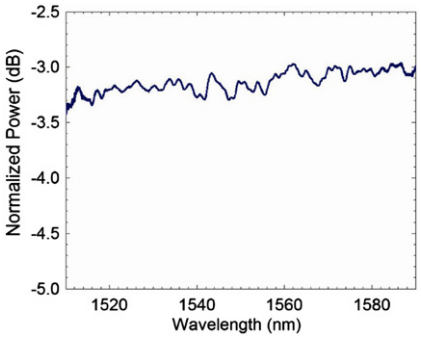

Fig. 6. Output spectrum of the 4×1 OPC normalized to the input erbium ASE spectrum. The OPC output spectrum is ~3 dB lower than that of the ASE source because of the connection, transmission, and coupling loss in the measurement setup.

5. Conclusion

In conclusion, highly-efficient optical power combiners, both incoherent and coherent, were proposed and experimentally demonstrated. Experimental results show that a high combining efficiency of $>90\%$ can be achieved. It should be noted that the geometrical parameters of the MNOFs, including waist diameter, tapering angle, and overlap length, all play key roles in power combination. Benefiting from their easy fabrication, high combining efficiency, wavelength-insensitivity and low cost, the MNOFs-based OPC can find potential applications in micro/nano photonic devices, interconnects, and optical networks.

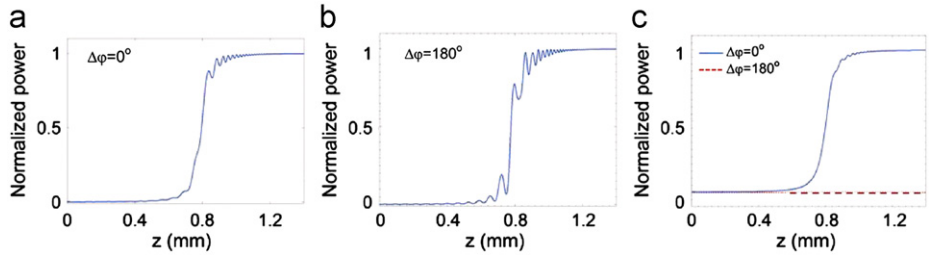

Fig. 7. Simulation results of the normalized power in the single MNOF of a 2×1 OPC along the propagation direction z. In (a) and (b), the input MNOFs have different cross-sectional dimension, and in (c), they are identical.

Acknowledgments

This work was supported in part by 973 program (ID2011CB301700), International Cooperation Project from Ministry of Science and Technology, P. R. China(2011FDA11780), NSFC (60877012, 61007039, 61007052, 61107041, 61127016), STCSM Project (10DJ1400402, 09JC1408100) State Key Lab Projects (GKZD030004/09/15/20/21), Shanghai Jiao Tong University Innovation Fund For Postgraduates.

References

[1] T. Shen, D. Rogovin, Physical Review Letters 61 (1988) 951.
[2] R. Uberna, A. Bratcher, B.G. Tiemann, IEEE Journal of Quantum Electronics 46 (2010) 1191.
[3] M. Yanxin, X. Wang, J. Leng, H. Xiao, X. Dong, Optics Letters 36 (2011) 951.
[4] F. Zhang, Q. Lou, J. Zhou, Y. Xing, W. Wang, Optik 120 (2009) 804.
[5] D. Noordegraaf, M.D. Maack, Proceedings of SPIE 7914 (2011) 79142L.
[6] P. Phua, Y.L. Lim, Optics Letters 31 (2006) 2148.
[7] J. Mu, C. Xu, W.P. Huang, Optics Express 17 (2009) 4791.
[8] H. Yamada, M. Nozawa, M. Kinoshita, Optics Express 19 (2011) 698.
[9] L. Tong, R.R. Gattass, J.B. Ashcom, S. He, J. Lou, Nature 426 (2003) 816.
[10] G. Brambilla, Journal of Optics 12 (2010) 043001.
[11] Y. Dong-Il, E.C. Mägi, R.E. Michael, Optics Letters 33 (2008) 660.
[12] Z. Zhe, L. Xin, Y. Zhang, Optics Letters 35 (2010) 974.
[13] M. Sumetsky, Y. Dulashko, J.M. Fini, A. Hale, Applied Physics Letters 86 (2005) 161108.
[14] P. Parama, H. Knox Wayne, IEEE Photonics Technology Letters 21 (2009) 766.
[15] Y. Wu, X. Zeng, H. Changlun, B. Jian, Applied Physics Letters 86 (2008) 191112.
[16] J. Xiaoshun, L. Tong, G. Vienne, Applied Physics Letters 88 (2006) 223501.
[17] M. Sumetsky, Optics Letters 35 (2010) 2385.
[18] H. Zehua, L. Xinwan, Z. Linjie, Optics Express 19 (2011) 3854.
[19] F.M. Davidson, C.T. Field, Journal of Lightwave Technology 12 (1994) 1207.
[20] C. Jianping, S. Xiaowei, H. Zehua, L. Xinwan, Proceedings of 15th OptoElectronics and Communications Conference (OECC2010) invited paper 8E2-1.
[21] P. Minhao, L. Liu, H. Ou, K. Yvind, J.M. Hvam, Proceedings of 36th European Conference and Exhibition on Optical Communication (ECOC2010) Tu.5.C.6.
[22] A. Hardy, W. Streifer, Journal of Lightwave Technology LT-3 (1985) 1135.